EXPERIMENTS AND NUMERICAL SIMULATIONS OF HORIZONTAL TWO PHASE FLOW REGIMES

Thomas HÖHNE[*]

Forschungszentrum Dresden-Rossendorf e.V.,

P.O. Box: 510119, 01314 Dresden, Germany

*Corresponding author, E-mail address: t.hoehne@fzd.de

ABSTRACT

Stratified two-phase flow regimes can occur in the main cooling lines of Pressurized Water Reactors, Chemical plants and Oil pipelines. A relevant problem occurring is the development of wavy stratified flows which can lead to slug generation. In the last decade, the stratified flows are increasingly modelled with computational fluid dynamics (CFD) codes. In CFD, closure models are required that must be validated. The recent improvements of the multiphase flow modelling in the ANSYS CFX code make it now possible to simulate these mechanisms in detail. In order to validate existing and further developed multiphase flow models, high-resolution measurement data is needed in time and also in space. For the experimental investigation of co-current air/water flows, the HAWAC (Horizontal Air/Water Channel) was built. The channel allows in particular the study of air/water slug flow under atmospheric pressure. Parallel to the experiments, CFD calculations were carried out. The two-fluid model was applied with a special turbulence damping procedure at the free surface. An Algebraic Interfacial Area Density (AIAD) model on the basis of the implemented mixture model was introduced, which allows the detection of the morphological form of the two phase flow and the corresponding switching via a blending function of each correlation from one object pair to another. As a result this model can distinguish between bubbles, droplets and the free surface using the local liquid phase volume fraction value. The behaviour of slug generation and propagation was qualitatively reproduced by the simulation, while local deviations require a continuation of the work. The creation of small instabilities due to pressure surge or an increase of interfacial momentum should be analysed in the future. Furthermore, experiments with pressure and velocity measurements are planned and will allow quantitative comparisons, at other superficial velocities.

NOMENCLATURE

a	-	blending coefficient
A	m^{-1}	interfacial area density
A	m²	projected area of the body in the direction of flow
B	-	model parameter (damping of turbulent diffusion)
C_D	-	dimensionless drag coefficient
d	m	bubble diameter
D_h	m	hydraulic diameter
F_d	N	drag force
g	ms^{-2}	gravity vector
h	m	channel height
J	ms^{-1}	superficial velocity
k	Jkg^{-1}	turbulent kinetic energy
L	m	channel length
n	-	typical grid cell size across the interface
P	kgs^{-2}	buoyancy production term (full buoyancy model)
Pr	-	Prandtl-number
r	-	volume fraction
$\dot{S}$	s^{-1}	strain-rate tensor
t	s	time
U	ms^{-1}	relative velocity between phases
x	m	x coordinate (channel width)
y	m	y coordinate (channel height)
z	m	z coordinate (channel length)
α	-	k-ω model closure coefficient of the generation term
β	-	k-ω model closure coefficient of the destruction term
ρ	kgm^{-3}	fluid density
σ_ω	-	inverse of the turbulent Prandtl number for ω
τ_t	Nm^{-2}	Reynolds stress tensor
μ	kg.m^{-1}s^{-1}	viscosity
ω	s^{-1}	specific dissipation

Indices

B	bubble
D	droplet
FS	free surface
G	gas
L	liquid
W	wall

INTRODUCTION

Stratified two phase flows occur in many industrial applications. The effects of the flow on the quantities (such as flow rate, pressure drop and flow regimes) always been of engineering interest. Wallis (1973) analysed the onset of slugging in horizontal and near horizontal gas-liquid flows. A prediction of horizontal flow regime transitions in pipes was introduced by Taitel and Dukler (1976). They explained the formation of slug flow by the Kelvin-Helmholtz instability. They also proposed a model for the frequency of slug initiation (1977). The viscous Kelvin-Helmholtz analysis proposed by Lin & Hanratty (1986) generally gives better predictions for the onset of slug flow. A general overview of the phenomenological modelling of slug flow was given by Hewitt (2003). Various multidimensional numerical models were developed to simulate stratified flows: Marker and Cell

(Harlow and Welch, (1965)), Lagrangian grid methods and Volume of Fluid method (Hirt and Nichols, (1981)) and Level set method (Sussman, (1994)). These methods are in principle able to accurately capture most of the physics of the stratified flows. However, they cannot capture all the morphological formations like small bubbles and droplets if the grid is not reasonable small enough. One of the first attempts to simulate mixed flows was presented by Ĉerne et al. (2001) who coupled the VOF method with a two-fluid model in order to bring together the advantages of the both analytical formulations. Issa and Kempf (2003) worked on multi-fluid simulation of slugging phenomena in horizontal channels and showed a mechanistic approach to the prediction of hydrodynamic slug initiation, growth and subsequent development into continuous slug flow in pipelines. A systematic study of numerical simulation of slug flow in horizontal pipes using the two fluid formulation was carried out by Frank (2003). It was shown that the formation of the slug flow regime strongly depends on the wall friction of the liquid phase. In simulations using inlet/outlet boundary conditions it was found, that the formation of slug flow regimes strongly depends on the agitation or perturbation of the inlet boundary conditions. Furthermore Frank showed that the length of the computational domain plays an important role in slug formation. However, the direct comparison between CFD calculations and measurements of the slug generation mechanisms and its propagation in horizontal pipes was not analysed. For the experimental investigation of air/water flows, HAWAC (Horizontal Air/Water Channel) with rectangular cross-section was built at Forschungszentrum Dresden-Rossendorf (FZD). Its inlet device provides defined inlet boundary conditions. The channel allows in particular the study of air/water slug flow under atmospheric pressure. Parallel to the experiments, CFD calculations were carried out (Vallée, C. and Höhne, T. 2008). The aim of the numerical simulations presented in this paper is the validation of prediction of the slug flow with newly developed and implemented multiphase flow models in the code ANSYS CFX (2008).

HAWAC

The Horizontal Air/Water Channel (HAWAC) (Fig. 1) is devoted to co-current flow experiments. A special inlet device provides defined inlet boundary conditions by a separate injection of water and air into the test-section. A blade separating the phases can be moved up and down to control the free inlet cross-section for each phase. This allows influencing the evolution of the two-phase flow regime. The cross-section of the channel are 100 x 30 mm² (height x width). The test-section is about 8 m long, and therefore the length-to-height ratio L/h is 80. Alternatively, related to the hydraulic diameter, the dimensionless length of the channel is $L/D_h = 173$. The inlet device (Fig. 1) is designed for a separate injection of water and air into the channel. The air flows through the upper part and the water through the lower part of this device. Because the inlet geometry produces a lot of perturbations in the flow (bends, transition from pipes to rectangular cross-section), four wire mesh filters are mounted in each part of the inlet device. The filters are made of stainless steel wires with a diameter of 0.63 mm and have a mesh size of 1.06 mm. They aim at providing

homogenous velocity profiles at the test-section inlet. Moreover, the filters produce a pressure drop that attenuate the effect of the pressure surge created by slug flow on the fluid supply systems. Air and water come in contact at the final edge of a 500 mm long blade that divides both phases downstream of the filter segment. The free inlet cross-section for each phase can be controlled by inclining this blade up and down. In this way, the perturbation caused by the first contact between gas and liquid can be either minimised or, if required, a perturbation can be introduced (e. g. hydraulic jump). Both, filters and inclinable blade, provide well-defined inlet boundary conditions for the CFD model and therefore offer very good validation possibilities. Optical measurements were performed with a high-speed video camera.
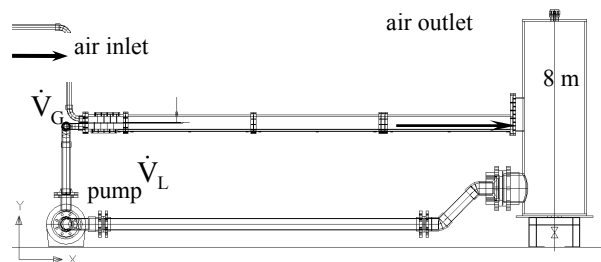

Figure 1: Schematic view of the horizontal channel HAWAC with inlet device for a separate injection of water and air into the test-section

FREE SURFACE MODELLING

The CFD simulation of free surface flows can be performed using the multi-fluid Euler-Euler modelling approach available in ANSYS CFX. Detailed derivation of the two-fluid model can be found in the book of Ishii and Hibiki (2006). However it requires careful treatment of several aspects of the model:

o   The interfacial area density should satisfy the integral volume balance condition. If surface waves are present, their contribution to the interfacial area density should be also taken into account.
o   The turbulence model should address the damping of turbulence near the free surface.
o   The interphase momentum models should take the surface morphology into account.

Turbulence damping at the free surface

As the goal of the CFD calculation was to induce surface instabilities, which are later generating waves and slugs, the interfacial momentum exchange and also the turbulence parameters had to be modelled correctly. Without any special treatment of the free surface, the high velocity gradients at the free surface, especially in the gaseous phase, generate too high turbulence throughout the two-phase flow when using the differential eddy viscosity models like the k-ε or the k-ω model. Therefore, damping of turbulence is necessary in the interfacial area. A few empirical models have been suggested, which address the turbulence anisotropy at the free surface, see among others Celik and Rodi (1984). However, no model is applicable for a wide range of flow conditions, and all of them are non-local: they require for example explicit specification of the liquid layer thickness, of the amplitude

and period of surface waves, etc. Menter (Yegorov, Y., Menter, F., 2004) proposed a simple symmetric damping procedure. This procedure provides for the solid wall-like damping of turbulence in both gas and liquid phases. It is based on the standard ω-equation, formulated by Wilcox (1994) as follows:

$$\frac{\partial}{\partial t}(\rho \cdot \omega) + \nabla \cdot (\rho \cdot U \cdot \omega) = \alpha \cdot \frac{\rho \cdot \omega}{k} \cdot \tau_t \cdot \dot{S} - \beta \cdot \rho \cdot \omega^2 + \nabla[(\mu + \sigma_\omega \cdot \mu_t) \cdot \nabla \omega]$$
(1)

where $\alpha = 0.52$ and $\beta = 0.075$ are the k-ω model closure coefficients of the generation and the destruction terms in the ω-equation, $\sigma_\omega = 0.5$ is the inverse of the turbulent Prandtl number for ω, τ_t is the Reynolds stress tensor, and $\dot{S}$ is the strain-rate tensor. In order to mimic turbulence damping near the free surface, Menter introduced a source term in the right hand side of the gas and liquid phase ω-equations. A factor activates a source term only at the free surface, where it cancels the standard ω-destruction term of the ω-equation $\left(-r_i \cdot \beta \cdot \rho_i \cdot \omega_i^2\right)$ and enforces the required high value of ω_i and thus the turbulence damping.

Algebraic Interfacial Area Density (AIAD) Model

Fig. 2 shows different morphologies at slug flow conditions. Separate models are necessary for dispersed particles and separated continuous phases (interfacial drag etc.). Two approaches are possible within the Euler-Euler methodology:

Figure 2: Different morphologies at slug flow conditions

o Four phases: Bubble/Droplet generation and degassing have to be implemented as sources and sinks
o Two phases: Momentum exchange coefficients depend on local morphology

For the second approach Yegorov (2004) proposed an Algebraic Interfacial Area Density (AIAD) Model. The basic idea of the model is:

o The interfacial area density allows the detection of the morphological form and the corresponding switching of each correlation from one object pair to another.
o It provides a law for the interfacial area density and the drag coefficient for full range $0 \le r_\alpha \le 1$.
o The model improves the physical modelling in the asymptotic limits of bubbly and droplet flows.
o The interfacial area density in the intermediate range is set to the interfacial area density for free surface

In an Euler-Euler simulation of horizontal slug flow the air entrainment below the water surface can be caused by the drag force. The magnitude of the force density for the drag is

$$|D| = C_D A \frac{1}{2} \rho |U|^2$$
(2)

where C_D is the drag coefficient, A the interfacial area density and ρ the density of the continuous phase (if the other phase is a dispersed phase). U is the relative velocity between the two phases. The AIAD model applies three different drag coefficients, $C_{D,B}$ for bubbles, $C_{D,D}$ for the droplets and $C_{D,FS}$ for free surface (Fig. 3). Non-drag forces (e.g. lift force and turbulent dispersion force) are neglected. The interfacial area density A also depends on the morphology of the phases. For bubbles it is

$$A = \frac{6r_G}{d_B}$$
(3)

where the interface area density is equal to the surface area of the spheres of diameter d_B, which occupy the gas volume fraction r_G.

For a free surface an important requirement for the model is the normalizing condition: the volume integral of the area density must be equal to the real surface area. It means that integration of the area density along a normal to the surface must yield unity:

$$\int_{-\infty}^{+\infty} A \, dn = 1$$
(4)

A model, which satisfies this condition, calculates the interface area density as the absolute value of the volume fraction gradient:

$$A_{FS} = |\nabla r_L| = \frac{\partial r_L}{\partial n}$$
(5)

if n is directed to the bulk liquid phase. For ρ the average density is applied, i.e.

$$\rho = r_G \rho_G + r_L \rho_L$$
(6)

where r_L and r_G are the liquid and the gas phase density respectively. In the bubbly regime, where a_G is low, the average density ρ is close to the liquid phase density ρ_L. According to the flow regime (bubbly flow, droplet flow or stratified flow with a free surface) the corresponding drag coefficients and interfacial area densities have to be applied (Fig. 2).

The simplest switching procedure for the interfacial area density, uses the blending function F_d. Introducing void fraction limits, the weights for flow regimes and length scales for bubbly and droplet flow (d_B, d_D) are the following:

$$f_B = \left[1 + e^{a_B(r_G - r_{B,limit})}\right]^{-1}$$
(7)

$$f_{FS} = 1 - f_B - f_D$$
(8)

$$A = f_{FS} A_{FS} + f_B A_B + f_D A_D$$
(9)

$$C_D = f_{FS} C_{D,FS} + f_B C_{D,B} + f_D C_{D,D}$$
(10)

Fig. 5 shows different blending functions f_B for different VF limits and blending coefficients. For the simulation of slug flow the void fraction limits of $r_{B,limit}=0.3$ resp. $r_{D,limit}=0.3$ and blending coefficients of $a_B=a_D=70$ are recommended.

Modelling the free surface drag

In simulations of free surface flows eq. (2) does not represent a realistic physical model. It is reasonable to expect that the velocities of both fluids in the vicinity of the interface are rather similar. To achieve this result, a shear stress like a wall shear stress is assumed near the surface from both sides to reduce the velocity differences of both phases (Fig. 3).
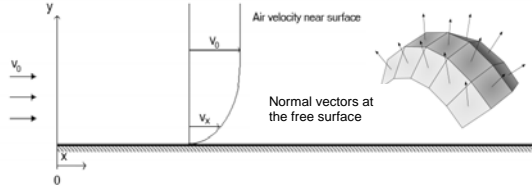

Figure 3: Air velocity near the free surface dependent on the normal vectors

A viscous fluid moving along a "solid" like boundary will incur a shear stress, the no-slip condition, the morphology region "free surface" is the boundary layer, the shear stress is imparted onto the boundary as a result of this loss of velocity

$$\tau_W = \mu \frac{\partial u}{\partial y}\Big|_{y=0} \qquad (11)$$

The components of the Normal vector at the free surface are taken from the gradients of the void fraction in x,y,z directions. As a result the modified drag coefficient is dependent on the viscosities of both phases, the local gradients of gas/liquid velocities normal to the free surface, the liquid density and the slip velocity between the phases:

$$C_D = \frac{2\left[r_L \tau_{W,L} + r_G \tau_{W,G}\right]}{\rho_L \cdot U^2} \qquad (12)$$

Boundary Conditions

The HAWAC channel with rectangular cross-section was modelled using ANSYS CFX. The model dimensions are 8000 x 100 x 30 mm³ (length x height x width) (Fig. 4a). The grid consists of 1.2×10^6 hexahedral elements. A slug flow experiment at a superficial water velocity of 1.0 m/s and a superficial air velocity of 5.0 m/s was chosen for the CFD calculations. In the experiment, the inlet blade was in the horizontal position. Accordingly, the inlet blade was modelled (Fig. 4a) and the inlet was divided into two parts: in the lower 50% of the inlet cross-section, water was injected and in the upper 50% air. An initial water level of $y_0 = 50$ mm was assumed for the entire model length (Fig. 4b). In the simulation, both phases have been treated as isothermal and incompressible, at 25°C and at a reference pressure of 1 bar. A hydrostatic pressure was assumed for the liquid phase. Buoyancy effects between the two phases are taken into account gravity. At the inlet, the turbulence properties were set using the "medium intensity and eddy viscosity ratio" option of the flow solver. This is equivalent to a turbulence intensity of 5% in both phases. The inner surface of the channel walls has been defined as hydraulically smooth with a non-slip

boundary condition applied to both gaseous and liquid phases. The channel outlet was modelled with a pressure controlled outlet boundary condition. The parallel transient calculation of 15.0 s of simulation time on 4 processors took 10 CPU days. A high-resolution discretization scheme was used. For time integration, the fully implicit second order backward Euler method was applied with a constant time step of $\Delta t = 0.001$ s and a maximum of 15 coefficient loops. A convergence in terms of the RMS values of the residuals to be less then 10^{-4} could be assured most of the time. The implementation of the AIAD model and turbulence damping functions into CFX was done via the command language CCL (CEL, Expressions) and User Fortran Routines.
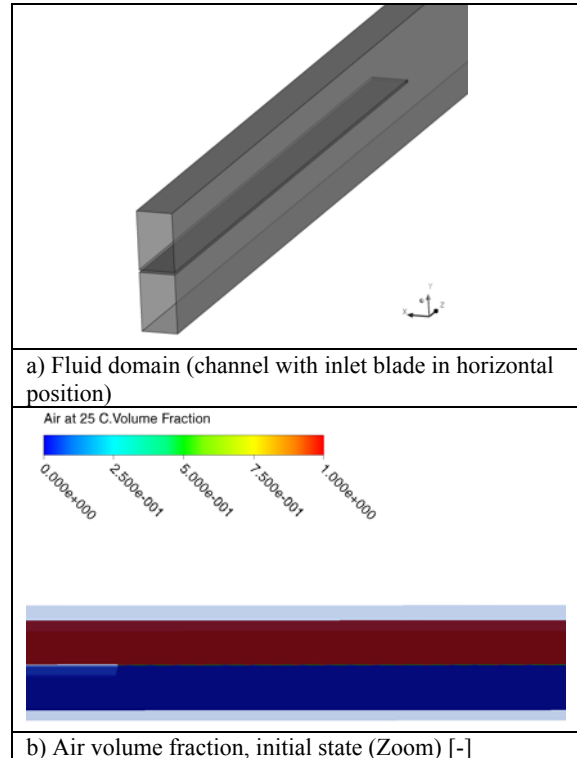

a) Fluid domain (channel with inlet blade in horizontal position)

b) Air volume fraction, initial state (Zoom) [-]

Figure 4: Model and initial conditions of the volume fractions

RESULTS: COMPARISON BETWEEN SIMULATION AND EXPERIMENT

A simulated free surface at the HAWAC channel with small surface instabilities is given in Fig. 6. Fig. 7 shows the resulting Interfacial Area Density variable. The AIAD model uses the following three different drag coefficients: $C_{D,B} = 0.44$ for bubbles, $C_{D,D} = 0.44$ for the droplets and $C_{D,S}$ according to the equations 11 and 12 for the free surface (see Fig. 8). In the picture sequences (Fig. 9 and 10) a comparison is presented between CFD calculation and experiment: the calculated phase distribution is visualized and comparable camera frames are shown. In both cases, a slug is generated. The sequences show that the qualitative behaviour of the creation and propagation of the slug is similar in the experiment and in the CFD calculation.
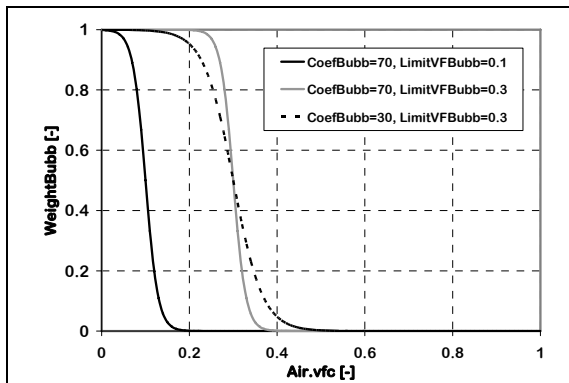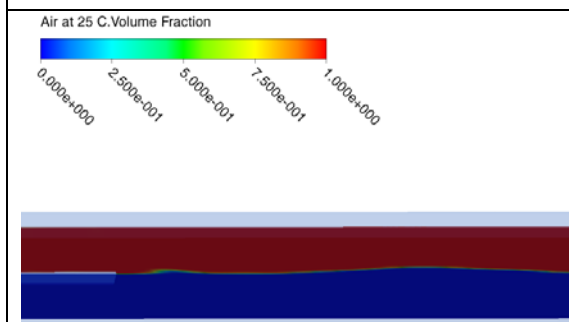
4

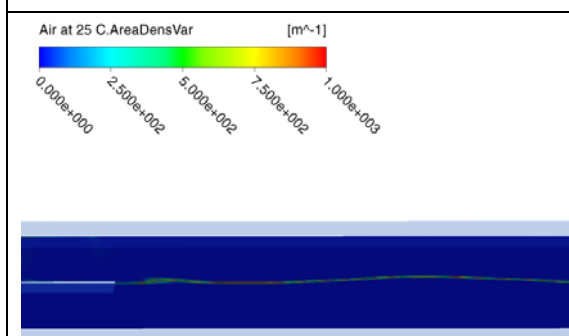**Figure 5**: Blending functions f_B blending coeff.

Figure 6: Air volume fraction [-]

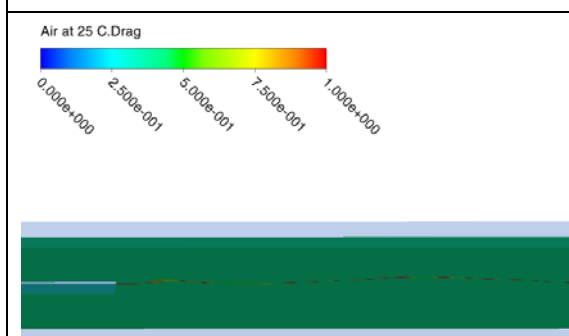**Figure 7:** Interfacial area density variable [m^-1]
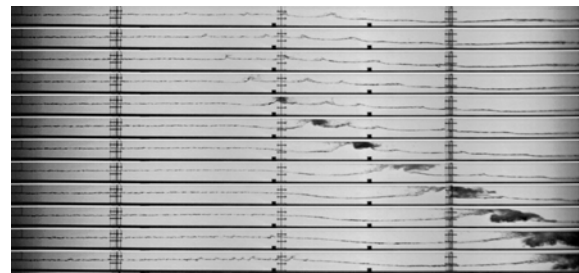

Figure 8: Drag coefficient [-]

Figure 9: Measured picture sequence at J_L = 1.0 m/s and J_G = 5.0 m/s with Δt = 50 ms (depicted part of the channel: 0 to 3.2 m after the inlet)

Figure 10: Calculated picture sequence at J_L = 1.0 m/s and J_G = 5.0 m/s (depicted part of the channel: 1.4 to 6 m after the inlet)

In the CFD calculation, the slug is induced by instabilities. The single effects leading to slug flow that can be simulated are:

o Instabilities and small waves are generated by the interfacial momentum transfer randomly. As a result bigger waves are generated.
o The waves can have different velocities and can merge together.
o Bigger waves roll over and can close the channel cross-section.

However, a detailed comparison shows quantitative deviations between simulation and measurement. The needed entrance length for slug generation was defined as the length between the inlet and the location nearest the inlet where a wave closes nearly the entire cross-section. This was observed at about 1.5 m in the experiment and 2.5 m in the calculation.

These quantitative differences can be explained with the flow regimes observed at the test-section inlet. In fact, the flow pattern has an important influence on the momentum exchange between gas and liquid, especially at high velocity differences between the phases. Small disturbances of the interface provide a more efficient momentum transfer from the air to the water than in a stratified smooth flow. A high momentum transfer induces a rapid wave growth and therefore slug generation. In this case, in the experiment supercritical flow waves were observed from the inlet of the channel. This means that the boundary conditions chosen for the CFD model do not reproduce all small disturbances observed in the experiment. In the end, a quite long channel length is needed before waves appear spontaneously in the simulation.

Future work should focus on the proper modelling of the small instabilities observed at the channel inlet.

CONCLUSION

In the HAWAC test facility, a special inlet device provides well defined as well as variable boundary conditions, which allow very good CFD-code validation possibilities. A picture sequence recorded during slug flow was compared with the equivalent CFD simulation made with the code ANSYS CFX. The two-fluid model was applied with a special turbulence damping procedure at the free surface. An Algebraic Interfacial Area Density (AIAD) model on the basis of the implemented mixture model was introduced and implemented. It improves the physical modelling, detection of the morphological form and the corresponding switching of each correlation is now possible. The behaviour of slug generation and propagation at the experimental setup was reproduced, while deviations require a continuation of the work. Experiments like pressure and velocity measurements are planned and will allow quantitative comparisons, also at other superficial velocities.

REFERENCES

ANSYS CFX, 2008. User Manual. Ansys Inc.

CELIK, I., AND RODI, W. 1984. A deposition-entrainment model for suspended sediment transport. Report SFB 210/T/6, Strömungstechnische Bemessungsgrundlagen für Bauwerke, University of Karlsruhe, Germany.

CERNE, G., PETELIN, S., TISELJ, I. 2001. Coupling of the interface tracking and the two-fluid models for the simulation of incompressible two-phase flow. Journal of Computational Physics 171 (2), 776-804.

FRANK, T. 2003. Numerical simulations of multiphase flows using CFX-5. CFX Users conference, Garmisch-Partenkirchen, Germany.

HARLOW, F. H., WELCH, J. E. 1965. Numerical calculation of time-dependent viscous incompressible flow of fluid with free surface. Physics of Fluids 8 (12), 2182-2189.

HEWITT, G. F. 2003. Phenomenological modelling of slug flow. Short course modelling and computation of multiphase flows, ETH Zurich, Switzerland.

HIRT, C. W., NICHOLS, B. D. 1981. Volume of fluid (VOF) method for the dynamics of free boundaries. Journal of Computational Physics 39 (1), 201-225.

ISHII, M., HIBIKI, T. 2006. Thermo-fluid Dynamics of Two-phase Flow. Springer-Verlag.

ISSA, R., KEMPF, , MHW. 2003. Simulation of slug flow in horizontal and nearly horizontal pipes with the two-fluid model, INT. J. MULTIPHAS. FLOW, Vol: 29, Pages: 69 – 95.

LIN, P. Y., AND HANRATTY, T. J. 1986. Prediction of the initiation of slugs with linear stability theory. Int. J. Multiphase Flow, 12, 79-98.

SUSSMAN, M. 1994. A level set approach for computing solutions to incompressible two-phase flow. Journal of Computational Physics 114 (1), 146-159.

TAITEL, Y., AND DUKLER, A. E. 1976. A model for predicting flow regime transitions in horizontal and near horizontal gas-liquid flow. AIChE J. 22, 47-55.

TAITEL, Y., AND DUKLER, A.E. 1977. A model for slug frequency during gas-liquid flow in horizontal and near horizontal pipes. Int. J. Multiphase Flow, 3, 585-596.

VALLÉE, C., HÖHNE, T., PRASSER, H.-M., SÜHNEL, T. 2008, Experimental investigation and CFD simulation of horizontal stratified two-phase flow phenomena. NED, Volume 238, Issue 3, March 2008, Pages 637-646

WALLIS, G. D., AND DOBSON, J. E. 1973. Onset of slugging in horizontal stratified air-water flow. Int. J. Multiphase Flow 1, 173-193.

WILCOX, D. C. 1994. Turbulence modelling for CFD. La Cañada, California: DCW Industries Inc.

YEGOROV, Y., MENTER, F. 2004. Contact condensation in stratified steam-water flow, EVOL-ECORA –D 07.